International Immunology, Vol. 19, No. 5, pp. 645–655
doi:10.1093/intimm/dxm030

Influenza A virus elevates active cathepsin B in primary murine DC

Timo Burster[1], Thierry Giffon[1], Martin E. Dahl[1,6], Pia Björck[2], Matthew Bogyo[2,3], Ekkehard Weber[4], Kutubuddin Mahmood[5,7], David B. Lewis[1] and **Elizabeth D. Mellins[1]**

[1]Department of Pediatrics, [2]Department of Pathology and [3]Department of Microbiology and Immunology, Stanford University School of Medicine, Stanford, CA 94305, USA
[4]Institute of Physiological Chemistry, Martin Luther University Halle-Wittenberg, Halle, Germany
[5]MedImmune Vaccines, Mountain View, CA 94043, USA

[6]Present address: Roche Palo Alto LLC, Palo Alto, CA 94304, USA
[7]Present address: Novavax, Inc. Malvern, PA 19355, USA

Keywords: Cathepsin B, dendritic cells, influenza A

Abstract

Dendritic cells (DCs) act as a first-line recognition system for invading pathogens, such as influenza A. The interaction of DC with influenza A virus results in DC activation via endosomal Toll-like receptors and also leads to presentation of viral peptides on MHC class II molecules. Prior work demonstrated that influenza A virus (A/HK×31; H3N2) infection of BALB/c mice activates lung DCs for antigen presentation, and that the enhanced function of these cells persists long after viral clearance and resolution of the virus-induced inflammatory response. Whether influenza A virus has acute or longer-lasting effects on the endo/lysosomal antigen-processing machinery of DCs has not been studied. Here, we show that antigen presentation from intact protein antigen, but not peptide presentation, results in increased T cell stimulation by influenza-exposed lung DCs, suggesting increased antigen processing/loading in these DCs. We find that cathepsin (Cat) B levels and activity are substantially up-regulated in murine lung DCs, harvested 30 days after A/HK×31 infection. CatB levels and activity are also increased in murine splenic and bone marrow-derived DCs, following short-term *in vitro* exposure to UV-inactivated influenza A virus. Modest effects on CatX are also seen during *in vivo* and *in vitro* exposure to influenza A virus. Using a cell permeable Cat inhibitor, we show Cats in influenza-exposed DCs to be functional and required for generation of a T cell epitope from intact ovalbumin. Our findings indicate that influenza A virus affects the MHC class II antigen-processing pathway, an essential pathway for $CD4^+$ T cell activation.

Introduction

Influenza is a single-stranded RNA (ssRNA) enveloped virus that expresses surface glycoproteins hemagglutinin (HA), neuraminidase (NA) and matrix protein as well as numerous internal proteins, including nucleoprotein, polymerase proteins and non-structural proteins (1). Influenza virus strains A, B and C are distinguished by differences in nucleoprotein and matrix proteins. Influenza A virus is further subdivided into subtypes based on variations in HA and NA, for example H3N2.

Influenza A virus infects the mucosal epithelial cells in the respiratory track of the host and causes acute respiratory disease. Influenza virus HA binds to sialated receptors on the cell surface of host cells, including respiratory track epithelial cells and dendritic cells (DCs), and is taken up into endosomal compartments. The acidic environment of endosomes induces a conformational change in HA, allowing the virus to fuse with the endosomal membrane and enter the cytoplasm (2). Thus, influenza antigens enter both the endosomal and the cytoplasmic compartments, accessing the MHC class II and MHC class I antigen presentation pathways, respectively.

Influenza A virus, having ssRNA, also activates DCs via Toll-like receptor (TLR)-7. This endosomal TLR is expressed by murine plasmacytoid dendritic cells (pDCs) and myeloid dendritic cells (mDCs). ssRNA recognition does not require active viral replication, and it is thought that viral ssRNA is delivered to the endo/lysosomal compartments after viral

Received 29 July 2006, *accepted* 23 February 2007

Correspondence to: T. Burster; E-mail: tburster@stanford.edu or E. Mellins; E-mail: mellins@stanford.edu

Transmitting editor: R. Medzhitov

Advance Access publication 19 April 2007

internalization (3). TLR7 ligation appears to be crucial for the murine DC response to live and inactivated influenza A (4).

We (M.E.D. and D.B.L.) demonstrated that thirty days after influenza A virus infection in a murine model, lung DCs showed increased stimulatory activity for $CD4^+$ T cells (5). Cell-surface levels of MHC class II and co-stimulatory molecules, such as CD40, CD80 and CD86, were increased on lung DCs at this time point, suggesting one explanation for their enhanced antigen-presenting cell (APC) function. We were interested in whether influenza A virus has additional effects on MHC class II antigen-presenting pathway that might contribute to their increased stimulatory capacity.

MHC class II molecules are expressed in the endoplasmic reticulum, where they interact with a trimer of invariant chain (Ii) and the resulting nonomer traffics to endosomal compartments. Upon arrival in endosomes, Ii is degraded to a nested set of class II-associated invariant chain peptide (CLIP) fragments. CLIP is exchanged for other endosomal peptides by the action of H2-DM (reviewed by Busch *et al.*) (6).

Antigens access endosomes through internalization from the extracellular environment or targeted delivery from other intracellular compartments. In endosomes, antigen undergoes several processing steps until it is suitable for loading on MHC class II molecules (7). These processing steps include unfolding, disulfide reduction (for antigens with internal disulfide bonds) and proteolysis. The most widely studied proteases in this machinery are the cathepsins (Cats), and they are classified into three different types according to the amino acid in their active site: the aspartate (CatD and CatE) (8–10), cysteine [C1: CatB, H, X and S and C13: asparagine-specific endoprotease (AEP)] (11–15) and serine proteases (CatG) (16, 17). After exposure to maturation signals, for example LPS, DC induce and convert several proteases such as CatL, CatS and AEP to their active form (17–20).

In this report, we show that influenza A virus infection has effects on components of the processing machinery in lung DCs. We also demonstrate that other DCs show similar changes after exposure to influenza A virus and confirm that the affected proteins are functionally important for presentation of an exogenous antigen.

Methods

Mice

BALB/cJ mice were purchased from Jackson laboratories. Thy1.1 BALB/c mice were purchased from MMRRC and bred in our facility. DO11.10 ovalbumin (OVA)-specific $\alpha\beta$ TCR-transgenic mice were bred on a BALB/c background in our facility. All animal experiments were approved by institutional protocols of Stanford University.

DC purification from influenza A-infected or control mice

DCs were isolated from the spleens of uninfected BALB/c mice or lung tissue of mice 30 days after intra-nasal inoculation with 240 HA units of HK×31 influenza A virus in allantoic fluid from chicken eggs diluted with PBS or, as a control, with virus-free normal allantoic fluid (NAF), as described (5). DCs were isolated from splenic or lung tissue of mice by mincing tissue followed by treatment with 300 U ml^{-1} type I collagenase (Worthington Biochemical, Lakewood, NJ, USA) and 100 U ml^{-1} DNase I (Sigma–Aldrich, St Louis, MO, USA) for 90 min in RPMI 1640 medium without serum. After filtration through nylon gauze to remove debris, the cells were re-suspended in RPMI 1640 medium with 10% FCS and incubated with CD11c mAb-coated paramagnetic microbeads and applied to an AutoMacs according to the manufacturer's instructions (Miltenyi Biotec, Auburn, CA, USA). The A/HK×31 influenza A virus is a recombinant between A/PR8/8/34 (H1N1) and A/Aichi/2/68 with the surface H3N2 glycoprotein of A/Aichi and the internal components of A/PR8 (21).

DC-mediated T cell proliferation assay

OVA-specific $CD4^+$ T cells were purified from the spleen and peripheral lymph nodes of DO11.10 Rag2−/− mice by magnetic cell sorting (MACS) with CD4 mAb-coated microbeads (Miltenyi Biotec). Purified $CD4^+$ T cells (1×10^5) were then cultured for 72 h in 96-well round-bottomed plates with 2×10^4 MACS-purified $CD11c^+$ lung DCs from previously (30d) infected (HK×31) or mock-infected mice and OVA (100 μg ml^{-1}) or $OVA_{323–339}$ peptide (5 μg ml^{-1}) in a volume of 200 μl. Cell proliferation was measured by pulsing cell cultures with [^{3}H] thymidine ([^{3}H]Tdr) (1 μCi per well) and determining incorporation during the last 18 h of incubation using a microbeta reader (PerkinElmer, Shelton, CT, USA).

In vitro exposure to influenza strains

Influenza virus A and B strains [cold-adapted (c.a.) A/Sydney/5/97 and c.a. B/Harbin/7/94], provided as a kind gift by MedImmune Vaccines, Inc. (Mountain View, CA, USA), were used for *in vitro* experiments. These strains were 6:2 genetic reassortants between (c.a.) master donor strains [c.a. A/Ann Arbor 6/60 (H2N2) or c.a. B/Ann Arbor 1/66] and strains that donated the HA and NA gene segments: A/Sydney/5/97 (H3N2) and B/Harbin/7/94-like virus, respectively (22). The reassortant strains were plaque titered on MDCK cells, with titers recorded as plaque-forming unit (pfu) per milliliter. For inactivation, the c.a. viruses were exposed to a UV source light for 30 min and titered to confirm complete inactivation. Spleen cells or DCs from BALB/c mice were treated (1 pfu per cell) with UV-inactivated c.a. influenza A/Sydney/05/97 or UV-inactivated c.a. influenza B/Harbin/7/94-like strain for 24 h in RPMI 1640 complete medium (GIBCO Life Technologies, Grand Island, NY, USA) and harvested after washing with PBS.

Determination of CatB activity

Hydrolysis of CatB activity was determined using a fluorogenic substrate, as previously described (23). Briefly, 100 μM of the fluorogenic substrate Z-FR-AMC (R&D Systems, Minneapolis, MN, USA) in buffer [0.1 M citrate, pH 5.0, 4 mM dithiothreitol (DTT), 4 mM aprotinin and 4 mM EDTA] and whole-cell lysate (lysis buffer: 10 mM Tris, pH 7.5, 150 mM NaCl and 0.5% NP-40) from uninfected or influenza A virus-infected DCs were mixed on ice. Liberated fluorescence (excitation 380 nm, emission 460 nm) was measured every 5 min with a Gemini XS multiwell fluorometer (Molecular Devices, Sunnyvale, CA, USA). The fraction of the emitted fluorescence that could be inhibited by addition of 10 μM CatB-specific inhibitor CA074 [*N*-(L-3 *trans*-propylcarbamoyloxirane-2-carbonyl)-L-isoleucyl-L-proline] (Caltag, Burlingame, CA, USA) was considered CatB activity.

Activity-based probes to visualize active cysteine proteases

Cells were lysed in lysis buffer (10 mM Tris, pH 7.5, 150 mM NaCl and 0.5% NP-40) and 10 μg of cell lysates were incubated with reaction buffer (50 mM citrate, pH 5.0 and 50 mM DTT) in the presence of biotinylated DCG-04 (24) for 1 h at room temperature. Reactions were terminated by the addition of SDS-reducing sample buffer and immediate boiling. Samples were resolved by 12% SDS–PAGE gel, and then transferred to a polyvinylidene difluoride-membrane and visualized using streptavidin HRP and the enhanced chemiluminescence-detection kit (Amersham Biosciences, Pittsburgh, PA, USA).

Western blot

Anti-Cat antiserum was generated against affinity-purified human CatB (rabbit anti-mouse CatB, E. Weber University Halle-Wittenberg, Halle, Germany) and purified CatB from human liver was purchased from Calbiochem (Calbiochem, San Diego, CA, USA). The monoclonal mouse anti-β-actin antibody was obtained commercially (Sigma–Aldrich). Cells were lysed in lysis buffer (10 mM Tris, pH 7.5, 150 mM NaCl and 0.5% NP-40), adjusted for equal total protein quantified by Bradford, resolved by SDS–PAGE and immunoblotted using published conditions (17).

Flow cytometric staining

Spleen cells or bone marrow (BM)-derived mDCs from BALB/c mice were incubated with blocking buffer (10% human AB serum, Caltag) for 10 min at room temperature and then incubated for 15 min with CD11c–FITC, CD45R–TC (Caltag) or MHC class II (clone 2G9, which recognizes I-A and I-E, BD PharMingen, San Diego, CA, USA) in blocking buffer, washed with PBS (1% BSA, Sigma–Aldrich). Cells were incubated for 20 min with BD Fix/Perm (Becton Dickinson, San Jose, CA, USA) and washed twice with BD Perm solution. Incubating the cells for 10 min with 10% human AB serum diluted in BD Perm solution blocked non-specific binding. Cells were then stained with rabbit anti-mouse CatB, rabbit anti-mouse CatD (E. Weber University Halle-Wittenberg) or the isotype controls for 20 min, washed twice with BD Perm solution and incubated for 10 min with the second antibody (goat anti-rabbit PE, Caltag). Cells were analyzed using a FACScan flow cytometer (Becton Dickinson). A total of 50 000 cells were collected using CellQuest Software (Becton Dickinson) and analyzed by FlowJo (Tree Star, Inc., Ashland, OR, USA).

Generation of BM-derived mDCs

Mouse DCs were prepared as previously described (25). In brief, total BM cells from BALB/c mice were obtained by flushing the femurs and tibia with PBS using a 23-gage needle. After washing and lysis of red cells, total leukocytes were re-suspended in complete RPMI 1640 (GIBCO Life Technologies) supplemented with 5% fetal bovine serum (Cambrex, Walkersville, MD, USA), 10 mM HEPES, 2 mM L-glutamine, antibiotics, 1 mM Na pyruvate, 0.1 mM non-essential amino acids, 5×10^{-5} M 2-mercaptoethanol (all from GIBCO) and 100 ng ml^{-1} rFlt3-L (PeproTech, Rocky Hill, NJ, USA). Cells were cultured at 1×10^6 cells ml^{-1} in six-well plates (Falcon, Franklin Lakes, NJ, USA) for 10 days. Cells that detached from the plates were gently collected and washed once in PBS. Cells were further incubated together with FcR-blocking antibodies (CD16/CD32, clone 2.4G2, BD PharMingen at 1 μg/1×10^6 cells) for 30 min on ice. After washing, cells were stained with antibodies specific for mDCs (CD11b–allophycocyanin–Cy7, PharMingen) and pDCs and $B220^+$ DCs (B220–allophycocyanin, PharMingen) were excluded. Propidium iodide was included to gate out dead cells. Cells were sorted using a FACSVantage (Becton Dickinson). Gates were set to exclude dead cells and debris. Purity was usually ≅96% (data not shown). Post-sort FACS analysis using directly fluorochrome-conjugated antibodies showed that all cells expressed the common DC marker CD11c and were immature based on low expression of $I\text{-}A^d$ and CD86 (data not shown).

APC functional analysis in vitro

APCs were purified from spleen of Thy1.1 BALB/c mice ($I\text{-}A^d$) and OVA-specific $CD4^+$ T cells (Thy1.2) were purified from lymph nodes and spleen of DO11.10 Rag2−/− mice. APCs (5×10^4) and $CD4^+$ T cells (1×10^5) were cultured with OVA (100 μg ml^{-1}) or $OVA_{323–339}$ peptide (5 μg ml^{-1}), with or without CA074-methyl ester (OMe) (10 μM, Caltag), CA074 (10 μM, Caltag) or CatG-specific inhibitor (200 nM, Calbiochem) (26), respectively, for 3–5 days at 37°C in a volume of 200 μl. Some of the cultured cells were exposed to LPS (1 μg ml^{-1}) or UV-inactivated c.a. A/Sydney influenza A virus (1 pfu per cell). Cells were re-stimulated with phorbol myristate acetate (20 ng ml^{-1}) and ionomycin (0.2 ng ml^{-1}) for 6 h at 37°C, with 10 μg ml^{-1} Brefeldin-A added for the last 4 h. Anti-Thy1.2 mAb (clone 5a-8, Caltag) and anti-CD4 mAb were used for detection of the DO11-10 cells, and intracellular IFN-γ was detected with a PE-conjugated mAb (clone XMG1.2, eBiosciences) using the Cytofix/Cytoperm kit (BD Biosciences).

T lymphocyte proliferation was determined using carboxyfluoresceine diacetate succinimidyl ester (CFSE) labeling. Purified $CD4^+$ T from DO11-10 Rag2−/− cells were washed twice in serum-free medium (RPMI 1640) and incubated with 0.5 μM CFSE for 15 min, washed twice and re-suspended in complete RPMI 1640. CFSE-labeled cells (1×10^5) were then cultured with 5×10^4 APCs and OVA (100 μg ml^{-1}) for 3–5 days at 37°C. The DO11-10 TCR was detected with an allophycocyanin-conjugated KJ1-26 clonotypic mAb and CD69 with a PE-conjugated mAb (clone H1.2F3), all from Caltag Laboratories. DO11-10 cells were analyzed for their surface expression of CD69 versus CFSE on a FACSCalibur flow cytometer (BD Biosciences). Data were analyzed using FlowJo software (Tree Star, Inc.).

Results

Lung DCs have enhanced presentation of intact protein antigen but not peptide antigen after influenza A virus infection

We (M.E.D. and D.B.L.) have shown that lung DCs isolated from mice that were previously (30d) inoculated with influenza A virus have increased stimulatory capacity for antigen-specific $CD4^+$ T cells when provided with intact protein as antigen (5). To assess the contribution of antigen

processing/peptide loading to this enhanced APC function, we chose to compare T cell stimulation after incubation of influenza-exposed DCs with intact OVA with stimulation after incubation with OVA peptide ($OVA_{323–339}$). To obtain influenza-exposed DCs, we used our previous approach. We administered influenza A virus strain HK×31 (H3N2) in allantoic fluid intra-nasally to BALB/c mice; control mice received an equivalent volume of identically diluted virus-free NAF. Lung DCs were harvested 30 days after viral or NAF administration and MACS purified, based on CD11c expression. Purified splenic OVA-specific $CD4^+$ T cells from DO11.10 (OVA-specific TCR) Rag2−/− transgenic mice were cultured for 72 h together with lung DCs, OVA (100 μg ml^{-1}) or OVA peptide (5 μg ml^{-1}) and T cell proliferation was assessed by the incorporation of [^{3}H]Tdr. As shown in Fig. 1, lung DCs from influenza-infected mice pulsed with OVA protein-stimulated enhanced OVA-specific T cell proliferation compared with control lung DCs from uninfected mice. In contrast, after pulsing with OVA peptide, lung DCs from previously infected mice did not mediate enhanced T cell proliferation, despite having increased levels of surface class II and co-stimulatory molecules, as previously shown (5). These findings imply that differences that increase the generation of OVA peptide–MHC complexes from intact antigen contribute to the enhanced T cell proliferation mediated by lung DCs from mice previously infected with influenza A virus. Notably, when exogenous OVA peptide is the source of antigen, the T cell stimulation is higher for both influenza-exposed and control DCs. This finding indicates that naturally processed OVA peptide is limiting for peptide–MHC complex generation when intact OVA protein is the source of antigen, and thus argues that changes in generation or loading of OVA peptide are critical to the increased $CD4^+$ T cell stimulation observed with the DCs from influenza A-infected mice. Our data also show that peptide presentation by DCs isolated from uninfected control mice is more effective, which likely reflects their increased capacity for peptide exchange at the cell surface, as predicted by increased H2-DM activity in DCs after microbial stimuli (27).

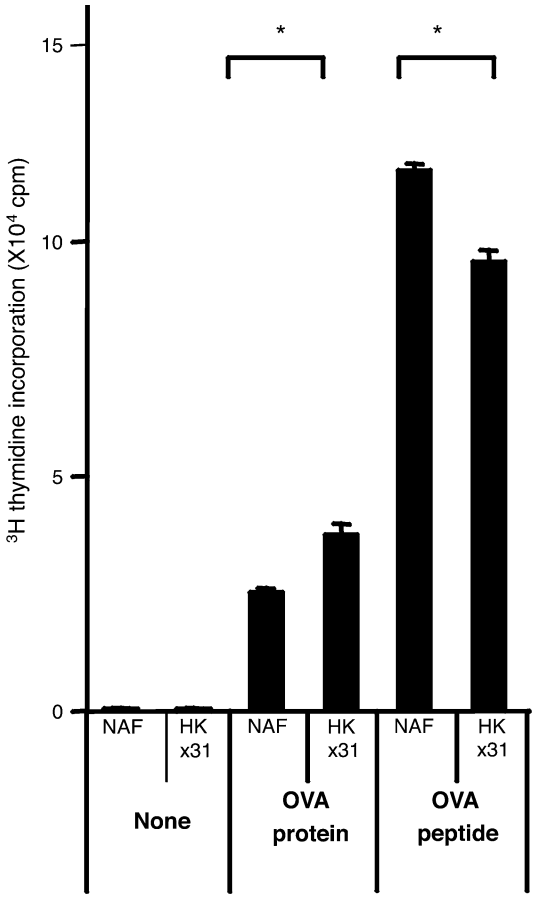

Fig. 1. Enhanced presentation of OVA protein but not peptide by lung DCs from influenza A virus-infected BALB/c mice. Lung DCs were purified from BALB/c mice previously (30d) infected with influenza A (HK×31) or treated with NAF as a control. Lung DCs were used as APCs to present either OVA protein or OVA peptide to OVA-specific $CD4^+$ T cells from DO11.10 Rag2−/− mice. T cell proliferation was assessed by the incorporation of [^{3}H]Tdr. One of two independent experiments with similar results is shown. *$P < 0.05$.

CatB is up-regulated in lung DCs from influenza A virus-infected mice

To pursue the implications of our findings on peptide versus protein presentation of OVA by lung DCs from influenza-infected mice, we chose to investigate Cat expression in lung DCs after influenza A HK×31 virus infection. We again administered virus or control NAF intra-nasally to BALB/c mice and 30 days after infection, lung DCs were isolated and purified from both infected and control mice. Cell lysates of lung DCs from both control and HK×31-infected mice were incubated with the biotinylated activity-based probe DCG-04 that labels cysteine Cats through an activity-dependent reaction with the active site thiol of these proteases. Thus, active-site labeling provides an indirect, but quantitative readout of protease activity. The lysates were loaded on a SDS–PAGE and visualized by streptavidin HRP blot (Fig. 2A). In lung DCs from both control and HK×31-infected mice, CatX was detected at a molecular weight of 35 kDa, CatB at 30 kDa, CatS at 25 kDa and CatL at 20 kDa in agreement with published data from BM-derived DCs (28). In lung DCs from HK×31-infected mice, there was a striking increase in levels of active CatB. Modest changes in CatX levels suggested an increase in this Cat as well. We also consistently noted an increase in an unknown (presumed) cysteine protease of apparent molecular weight around 40 kDa. However, no significant increase in levels of active forms of CatH, CatS and CatL was found in lung DCs from HK×31-infected mice compared with control-treated mice. β-Actin levels were measured to confirm that the same amount of protein was loaded on SDS–PAGE from experimental and control DC lysates.

Next, we measured the turn over of the fluorogenic substrate Z-FR-AMC in lung DCs from both control and HK×31-infected mice; substrate Z-FR-AMC detects CatB and CatL activity at pH 5.0. The substrate turn over was higher when we used lung DC lysate from HK×31-infected mice compared with lung DC lysate from control-treated mice (Fig. 2B), consistent with an increase in CatB activity in these cells. The relatively modest extent of the difference in cells from infected versus uninfected animals likely reflects the fact that CatL activity is also measured by this substrate,

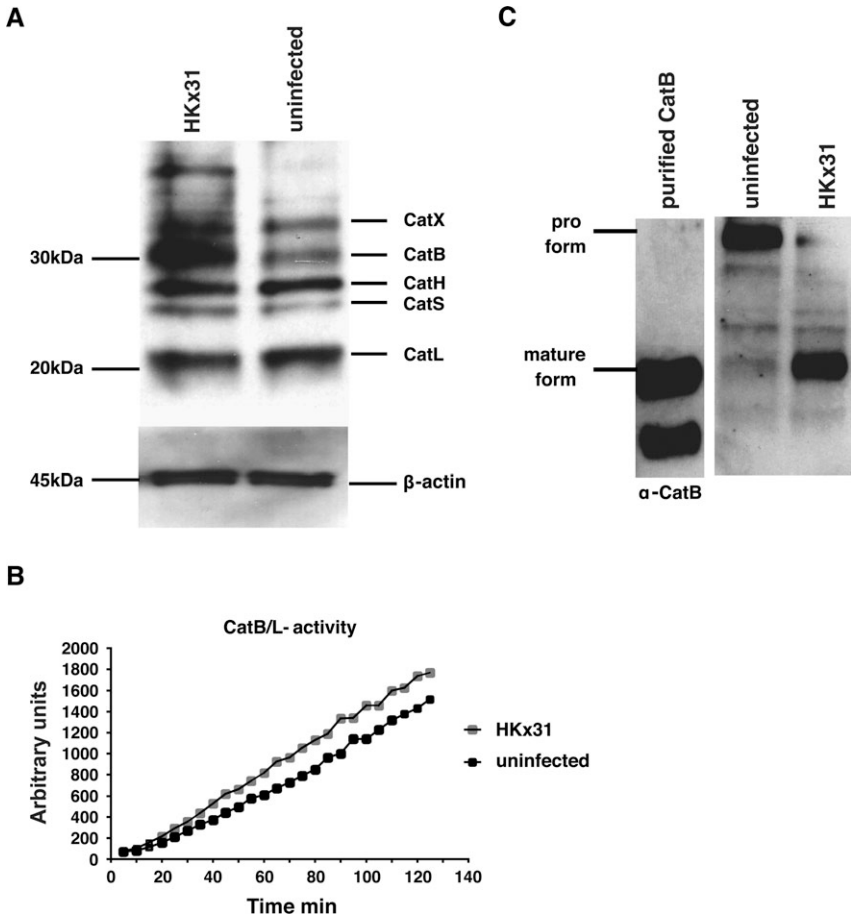

Fig. 2. CatB is up-regulated in purified lung DCs derived from influenza A (HK×31)-infected mice compared with control mice. (A) Cell lysates from purified lung DCs of virus-free NAF control or influenza A virus (HK×31)-inoculated mice were normalized for total protein content, labeled with the biotinylated activity-based probe DCG-04, resolved by SDS–PAGE and papain-like cysteine proteases were visualized by streptavidin HRP blot. β-Actin immunoblot was performed as a loading control. Data are representative of two experiments. (B) CatB/L activity was determined at pH 5.0 by measuring the turn over of the fluorogenic substrate Z-FR-AMC in cell lysates from purified lung DCs of control and influenza A virus (HK×31)-inoculated mice. (C) CatB protein levels in cell lysates from purified DCs from indicated mice were assessed by western blot with CatB-specific antibody. Purified recombinant CatB is used as a positive control.

and this activity is present in cells from both control and infected mice.

We also investigated the changes in total CatB levels by western blot, using an antibody that recognizes both proform (inactive) of CatB and the mature, active form. The same amount of protein from lung DCs from control and HK×31-infected mice was analyzed by SDS–PAGE, and CatB protein was detected (Fig. 2C). We observed striking differences in the relative levels of the mature and proforms of CatB. Mature CatB protein was predominant in lung DCs from HK×31-infected mice, while the proform of CatB was predominant in lung DCs from control-treated mice. We conclude that there is an increase in the amount of active CatB in lung DCs 30 days after HK×31 infection, and that this is likely due to the turn over of inactive proform CatB to active CatB.

Both splenic and BM-derived murine DCs increase levels of active CatB after exposure to UV-inactivated influenza A virus in vitro

We were interested to determine whether *in vitro* exposure to influenza virus affects CatB levels and activity in DCs acutely or whether this effect requires longer term exposure of DCs to the environment of the infected lung. To investigate this, we exposed freshly isolated spleen cells or purified CD11c$^+$ splenic DCs from BALB/c mice to influenza A virus. To avoid cell lysis, which arises during influenza infection, we used UV-inactivated influenza A or B viruses. Splenic DCs from BALB/c mice were incubated with a UV-inactivated influenza A virus strain that, like A/HK×31, expresses H3N2 [c.a. A/Sydney (H3N2); see Methods] at 1 pfu per cell or with UV-inactivated influenza B virus (c.a. B/Harbin-like) at 1 pfu per cell for 24 h *in vitro*. The DCs were harvested, and cell lysates were incubated with the activity-based label DCG-04 before analysis by SDS–PAGE. The active polypeptide CatB was visualized ~30 kDa and was dramatically increased in influenza A virus-exposed spleen DCs, while influenza B virus had only limited effects on CatB expression (Fig. 3A). CatH, CatS and CatL were hardly affected by influenza A virus, but CatX was modestly increased. Thus, we observed similar effects on these Cats in splenic DCs after acute exposure to UV-inactivated influenza A virus to those seen after influenza A infection in the whole animal, with up-regulation

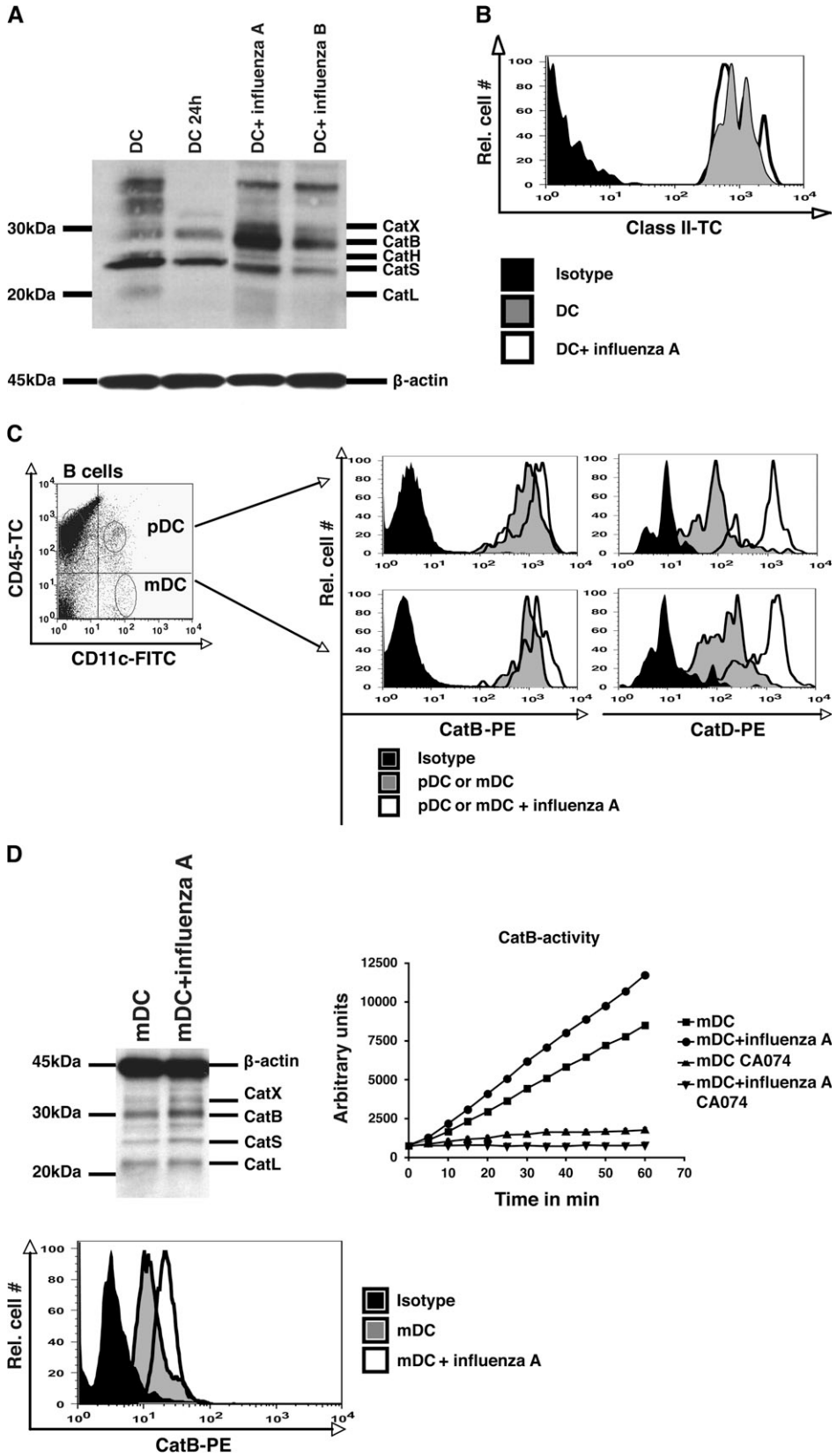

Fig. 3. CatB is up-regulated in both spleen and BM-derived DCs from BALB/c mice after exposure to UV-inactivated influenza A virus *in vitro*. (A) Active papain family cysteine proteases were measured in cell lysates from purified splenic DCs exposed for 24 h to UV-inactivated influenza A virus or mock-exposed cells, as a control. Cell lysates were incubated with activity-based cysteine protease probe, DCG-04, and comparable

of CatB being especially notable. Interestingly, however, when we exposed splenocytes to UV-inactivated influenza A and stained with MHC class II-specific antibody, recognizing I-A and I-E, and analyzed the MHC class II cell-surface expression of $CD11c^+$ gated cells by FACS, both influenza A-exposed DCs and control DCs had comparable MHC class II cell-surface expression (Fig. 3B), unlike DCs isolated from control versus influenza A-exposed animals at 30d. This result suggests that influenza-related effects on class II expression in DCs require different kinetics or mediators than effects on Cats.

DCs are divided into two subsets, mDC and pDC, and can be distinguished by the co-expression of distinct cell-surface markers. Murine mDC expresses CD11c and CD11b molecules, whereas murine pDC expresses CD11c and B220/CD45R. Next, we used FACS analysis to measure CatB and CatD levels in both mDC and pDC. Splenic DCs from BALB/c mice were exposed to UV-inactivated influenza A for 24 h, stained with CD11c–FITC and CD45–TC and, after permeabilization, stained intracellularly with anti-CatB or anti-CatD antibodies, which recognize both proform and active form. $B220/CD45R^+$ and $CD11c^{low}$ cells represent the pDCs, while $CD45R^-$ and $CD11b/CD11c^{high}$ cells are mDCs. Figure 3(C) shows the histograms for CatB or CatD protein, gated for pDCs and mDCs, as indicated. The solid histogram shows the isotype control, the tinted histogram indicates CatB or CatD levels in control splenic DCs and the unfilled histogram denotes splenic DCs exposed to influenza A. Control pDCs had less total CatB and CatD than influenza A virus-exposed pDCs, and the control mDCs had less total CatB and CatD than influenza A virus-exposed mDCs. The extent of the increase in total CatD was substantially greater than for CatB in both cell types. Thus, both mDCs and pDCs appear to be comparably affected, and total CatB and CatD levels are increased in both populations.

We also investigated the impact of exposure to UV-inactivated influenza A virus on CatB levels and activity in BM-derived DCs. BM cells from BALB/c mice were cultured in the presence of rFlt3-L for 10 days. Sorted mDCs were exposed to influenza A for 24 h. In Fig. 3(D), the left panel shows labeling by the activity-based probe. Active CatB was increased in influenza A virus-exposed cells and CatX was possibly increased to a minor extent, but changes in other Cats were not detected. The β-actin blot was used as a loading control. We also detected an increase in CatB when we performed intracellular staining with a CatB-specific antibody of control and influenza A virus-exposed mDCs and then analyzed by FACS. Increased CatB protein was detected in mDCs after influenza A virus exposure (unfilled histogram, median 20.7) compared with control mDCs (tinted histogram, median 11.7). The solid histogram represents the isotype control (Fig. 3C, lower panel).

To quantify the increase in CatB activity in BM-derived DCs after influenza A virus exposure, we used the fluorogenic substrate Z-FR-AMC (Fig. 3C, right panel). In addition, we included the CatB-specific inhibitor CA074 (end concentration 10 μM) in a separate reaction to assess the component of the total enzyme activity attributable to CatB. Increased substrate turn over was detected in cell lysates of mDCs after influenza A virus exposure, reflecting increased CatB activity. No substrate turn over was detected after addition of the CatB-specific CA074 inhibitor. These results demonstrate that primary as well as *in vitro* generated DCs can up-regulate CatB after exposure to UV-inactivated influenza A virus.

The inhibitor, CA074-OMe, reduces T cell proliferation

Active-site labeling of CatB indicated active protease in influenza A-exposed splenic DCs, but is an indirect measure of functional activity. To corroborate those results with a functional assay, we investigated processing and presentation of OVA peptide ($OVA_{323–339}$) by influenza-exposed and control DCs and the generation of $OVA_{323–339}$ is known to require CatB for processing from intact protein (29). APCs (T-depleted spleen cells) from BALB/c mice were treated *in vitro* with UV-inactivated influenza A or mock treated for 24 h and then were incubated for 5 days with native OVA as antigen. As another microbial stimulus, we also pre-incubated some APCs with LPS. The response of $I\text{-}A^d$-restricted, OVA-specific T cells purified from spleens of DO11.10 Rag2−/− OVA-specific mice was measured in a T cell proliferation assay. To directly test the role of CatB in our assay, some APC/T cell/OVA protein cultures were simultaneously incubated with a cell permeable inhibitor CA074-OMe, a non-cell permeable CatB-specific inhibitor (CA074) or a CatG inhibitor as another control. CA074 [*N*-(L-3 *trans*-propylcarbamoyloxirane-2-carbonyl)-L-isoleucyl-L-proline] is an epoxy–peptide-based inhibitor that specifically inactivates CatB, but cannot penetrate the cell membrane due to its negatively charged carboxylate group. In contrast, the methylated version, CA074-OMe, is inactive, but can traverse the cell membrane. In the cytosol, CA074-OMe is

amounts of total protein from each were analyzed by SDS–PAGE. β-Actin immunoblot was performed as a loading control. (B) Splenocytes were surface stained with antibody to MHC class II molecules that recognizes both I-A and I-E molecules and isotype control, as well as with anti-CD11c antibody to detect DCs. Stained cells were analyzed by FACS. (C) Whole splenocytes were exposed to UV-inactivated influenza A virus for 24 h, stained with CD45R–TC- and CD11c–FITC-conjugated antibodies, permeabilized and stained with anti-CatB–PE or anti-CatD–PE. Stained cells were analyzed by FACS, with gating for pDCs ($CD45R^+$ and $CD11c^+$) or mDCs ($CD11c^{+high}$). Splenocytes exposed to UV-inactivated influenza A virus are indicated by the unfilled histogram, control cells by the tinted histogram and the isotype control by the black histogram. Data are representative of three independent experiments. (D) Upper left panel: BM-derived DCs were obtained from total BM from BALB/c mice, and cultured with rFlt3-L for 10 days; cells were purified and exposed to UV-inactivated influenza A virus for 24 h. Control and BM-derived DCs exposed to UV-inactivated influenza A virus were pre-incubated with the activity-based cysteine protease probe, DCG-04.Upper right panel: equal amounts of cell lysate from control and UV-inactivated influenza A virus-exposed BM-derived DCs, as indicated, were compared for their ability to turn over the fluorogenic substrate Z-FR-AMC. The CatB-specific inhibitor CA074 (10 μM) was used, as indicated, to determine the component of enzyme activity attributable to CatB. Lower left panel: FACS analysis was performed after intracellular staining with CatB-specific antibody. The unfilled histogram indicates BM-derived DCs exposed to UV-inactivated influenza A virus and tinted histogram indicates control BM-derived DCs. The solid black histogram represents the isotype control.

de-esterficated to generate the CatB-specific inhibitor CA074. However, because the intracellular conversion of CA074-OMe to the CatB-specific inhibitor CA074 is slow, we cannot rule out that other papain family cysteine proteases, such as CatL, may also be inhibited by the OMe. OVA-specific T cells were analyzed for their production of IFN-γ by intracellular staining followed by FACS analysis (Fig. 4A). Consistent with prior results, an increased proportion of T cells produced IFN-γ production in the presence of DCs treated with microbial stimuli and this increase was greater for influenza A virus-treated compared with LPS-treated DCs. In contrast, in presence of the cell permeable inhibitor CA074-OMe, IFN-γ production was reduced to background level, indicating that functional CatB was expressed by these cells and had access to the endocytosed OVA. Neither the non-cell permeable CatB inhibitor CA074 nor a CatG inhibitor affected T cell proliferation. In addition, Fig. 4(B) (upper panel) shows that, while IFN-γ production was decreased to background level using CA074-OMe and OVA protein, IFN-γ production was not decreased by using OVA peptide ($OVA_{323–339}$) and CA074-OMe. These results indicate that CA074-OMe was not cytotoxic for T cells, but was blocking an intracellular activity that is required for T cell stimulation.

As a second assay to evaluate T cell responses to OVA protein after exposure to influenza A, we evaluated T cell proliferation by dilution of CFSE label. Influenza A virus-treated APCs were more effective in inducing proliferation of OVA-specific T cells compared with untreated APCs (Fig. 4C). In contrast, in the presence of CA074-OMe inhibitor, activation

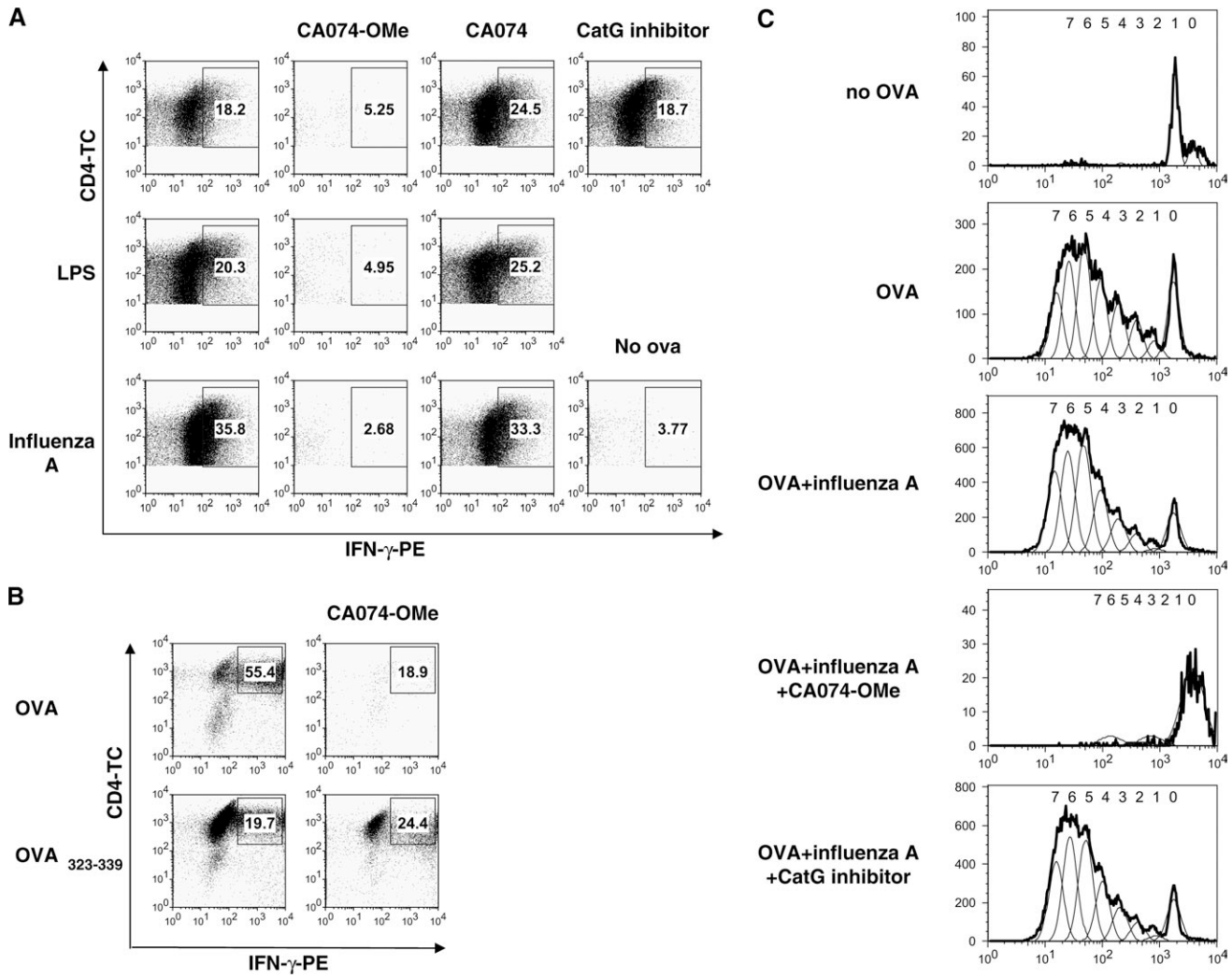

Fig. 4. The cell permeable Cat inhibitor CA074-OMe blocks presentation of OVA protein by influenza A virus-exposed APCs. (A) Whole splenocytes from BALB/c mice were exposed to UV-inactivated influenza A virus treated with LPS for 24 h or left untreated and then incubated with OVA protein, with and without the cell permeable (CA074-OMe, 10 μM), the non-cell permeable (CA074, 10 μM) CatB-specific inhibitor or a CatG-specific inhibitor for 5 days. IFN-γ production of T cells (Thy1.2) from DO11.10 Rag2−/− OVA-specific mice was determined by intracellular staining with IFN-γ-specific antibody and FACS analysis. Cells were cultured without OVA as a control. (B) Splenocytes from BALB/c mice were cultured with OVA peptide or OVA protein in the presence or absence of the inhibitor CA074-OMe (10 μM) (upper panel). IFN-γ production of T cells (Thy1.2) from DO11.10 Rag2−/− OVA-specific mice was determined by intracellular staining with IFN-γ-specific antibody and FACS analysis. (C) T cell proliferation was determined by reduction of CFSE label. Data are representative of three independent experiments.

of these cells was greatly decreased. Taken together, our results show that papain family cysteine proteases (most likely CatB) are functional in these cells, and indeed, are critical for the generation of the $OVA_{323–339}$ epitope, as has been observed for other APCs (29, 30).

Discussion

DCs are critical APCs that bridge innate and adaptive immune responses and uniquely prime naive T cells. In the present study, we found the capacity to stimulate T cells by lung DCs from influenza-infected mice was enhanced when antigen was provided as intact protein but not peptide, arguing for an effect of influenza infection on the antigen-processing/presentation machinery of lung DCs. We therefore investigated the influence of influenza A virus on Cat expression and activity in primary DCs. We found that (i) active CatB was up-regulated in lung DCs of previously influenza A virus-infected mice compared with lung DCs from uninfected control mice and (ii) freshly isolated as well as in BM-derived, cultured murine DCs also up-regulated active CatB after influenza A virus exposure. Using a CatB inhibitor, we were able to show that the CatB in influenza-exposed DCs was able to access endocytosed OVA protein and was required for its natural processing into the $OVA_{323–339}$ peptide. Overall, our functional studies of DCs exposed to influenza *in vivo* (Fig. 1) and *in vitro* (Fig. 4) argue that increased active CatB plays a role in the enhanced APC function of these cells. However, our studies cannot definitively isolate the contribution of the increased amount of active CatB in the influenza-treated APCs to their increased ability to stimulate T cells, because multiple changes occur in these cells.

We also observed that the increased CatB activity is associated with an increased conversion from proform to active CatB, which is likely triggered by other proteases. However, there are conflicting data in the literature regarding the processing of the proform to the active form of CatB. In one report, this processing event was inhibited when an aspartate protease inhibitor pepstatin A was used, suggesting that the aspartate protease CatD is a candidate for this function (31). Different results were obtained by Hara *et al.* (32), who used a metalloprotease inhibitor and proposed that a metalloprotease converted proform CatB to the active form. Yet a third study used diverse inhibitors, such as inhibitors of serine proteases (PMSF), aspartate proteases (pepstatin A) and cysteine proteases (E64-d); only E64-d treatment had an effect on the conversion from proform to active CatB (33). We found here that the active form of CatB was substantially increased in influenza A virus-exposed DCs, CatX was modestly increased and the level of several other active forms of cysteine proteases were unchanged. In addition, we observed increased total intracellular CatD expression by FACS in splenic DCs after influenza A virus exposure. It is possible that induction of CatD is necessary to convert the proform to the active form of CatB. Alternatively, access of CatD or other proteases, including those whose levels do not change, to the proform of CatB is changed in affected DCs, resulting in generation of mature, active CatB.

The carboxypeptidase CatX was previously determined to be present in APCs, such as macrophages and DCs, and is therefore hypothesized to be involved in antigen processing (28). Recent findings also suggest that CatX plays a role in T cell activation via regulation of the β_2-integrin leukocyte function-associated antigen-1 receptor (28, 34). We found that CatX activity was modestly increased in several types of DCs exposed to influenza A virus (Figs. 2A, 3A and C). Kos *et al.* (35) found that the total level of CatX was unchanged after maturation of human monocyte-derived DCs stimulated with tumor necrosis factor-α, but did not measure levels of active enzyme. In addition to this difference, both the target DC subtype and the maturation stimuli are different in the system of Kos *et al.* versus ours; a critical variable may be that influenza A virus stimulates a cytokine milieu that includes high levels of IFN-α. Thus, along with its function, the regulation of CatX upon DC maturation will be of interest to study further in various DC subsets.

It is interesting that influenza-mediated changes in the cysteine Cats are relatively selective for CatB. Active CatB can mediate destruction of perforin (36). After stimulation by antigenic peptide presented on MHC class I molecules, cytotoxic T cells up-regulate surface CatB, which has been proposed as a mechanism of protection against self-destruction by perforin (36). Peptide antigen-loaded DCs have been shown to be subject to CTL-mediated elimination after they have initiated an immune response in a murine model system (37). We reasoned that virus-exposed DCs might up-regulate surface CatB to bypass destruction by CTL. We looked at the cell-surface expression of CatB in control and influenza A virus-exposed splenic DCs, and detected CatB on the cell surface of pDCs as well as mDCs by FACS analysis. However, we did not observe any difference in cell-surface CatB expression after influenza A virus exposure on either pDCs or mDCs (data not shown). We also failed to detect active cysteine proteases in the supernatants from co-cultures of influenza A virus-exposed DCs with antigen and T cells (data not shown), suggesting that CatB was not secreted.

In addition, it was previously reported that CatB plays a crucial role in processing of the hepatitis B core antigen (38). Thus, we also considered the possibility that CatB is induced in order to degrade a critical influenza antigen, such as HA, one of the immunodominant influenza proteins. We exposed purified HA to B lymphoblastoid cell-derived lysosomal proteases and isolated human CatB *in vitro* and found that while lysosomal proteases can degrade HA, isolated human CatB alone is not sufficient (data not shown). The possibility that increased CatB improves the efficiency of HA processing remains to be explored.

The TLRs expressed by DCs allow for recognition of foreign viral and bacterial antigens (39, 40). Blander *et al.* (41) show that TLR signaling might regulate Cat activity, as increased Ii (p31) processing takes place in DC phagosomes exposed to microbial TLR ligands, but not phagosomes encountering antigen without TLR ligands. We observe that CatB activity is up-regulated after influenza A virus infection, and this change in CatB activity is also induced by UV-inactivated influenza A virus. This finding suggests the possible involvement of TLR signaling in our results. A candidate pathway is TLR7 recognition of ssRNA (3). An alternative, but not mutually exclusive, possibility is that HA protein may activate DCs, as we noted a difference in the

effects of influenza A and B strains *in vitro*, and there is a recent evidence for HA-mediated initiation of innate activation in B cells via a MyD88-dependent pathway that appears to use a novel receptor (42). Another viral protein, human papilloma virus type 16 E7, has been shown to increase CatB activity, resulting in induction of apoptosis (43).

In the setting of *in vivo* infection with influenza A virus, another possible contributor to the alterations in CatB is IFN-γ. It is known that lung infection with influenza A results in high local IFN-γ produced by $CD4^+$ T cells (5), and, more acutely, IFN-γ is produced by NK cells (44). In our *in vivo* system, using IFN-γ-deficient mice or IFN-γ neutralization, we were unable to observe influenza A virus-enhanced DC function, thus demonstrating an important role for IFN-γ in the cytokine milieu that mediates the persistent effects on lung DCs (5). It has been shown that IFN-γ and LPS stimulate increased CatB activity in human monocyte-derived DCs (17).

We found that the cell permeable inhibitor CA074-OMe reduced DO11.10 T cell proliferation. These results highlight the importance of papain family of cysteine proteases, most likely CatB, and not aspartate or serine proteases in the generation of $OVA_{323–339}$ peptide, the ligand required to stimulate these T cells. In contrast, the non-cell permeable CatB-specific inhibitor CA074 did not effect T cell stimulation in our system. Mizuochi *et al.* (29) found that CA074 decreased IL-2 production by T cells after APCs were pulsed with OVA protein, but not with $OVA_{323–339}$ peptide. However, Mizuochi *et al.* (29) used a B cell lymphoma as APC, whereas we have used primary DC, which may account for this discrepancy. It has also been reported that the presence of CA074 during stimulation with hepatitis B, *Leishmania major* antigen or OVA induces a switch of cytokine production from T_H2 to T_H1 type cytokines (30, 45, 46). This seems unlikely to account for our results, however, as we observed a striking block in proliferation of naive T cells by using CA074-OMe. Last, CA074-OMe was shown to reduce cell death in oral squamous carcinoma cells (47), consistent with our finding that CA074-OMe is not directly toxic to cells.

In conclusion, our findings indicate that influenza A virus increases CatB activity in freshly isolated DCs and suggest that altering this antigen-processing machinery may be a key effect of encounter with influenza A virus by these cells. As this effect appears to be relatively long-lived in lung DCs, it may contribute to enhanced processing and presentation of other antigens, including allergens, after influenza infection.

Acknowledgements

This work was supported by the National Institutes of Health (NIH) U54 AI057229 (to E.D.M.), the Deutsche Forschungsgemeinschaft BU 1822/1-1 and BU1822/3-1 (to T.B.), the Stanford University Immunology Training grant AI07290-19 (to M.E.D.), the American Lung Association grant RT-017-N (to M.E.D.) and the NIH National Technology Center for Networks and Pathways grant U54 RR020843 (to M.B.). We thank P. Doherty (University of Melbourne, Victoria, Australia) for providing HK×31 influenza A virus and control allantoic fluid and MedImmune Vaccines for the c.a. influenza strains and control allantoic fluid.

Abbreviations

AEP	asparagine-specific endoprotease
APC	antigen-presenting cell
BM	bone marrow
c.a.	cold adapted
Cat	cathepsin
CFSE	carboxyfluoresceine diacetate succinimidyl ester
CLIP	class II-associated invariant chain peptide
DC	dendritic cell
HA	hemagglutinin
Ii	invariant chain
MACS	magnetic cell sorting
mDC	myeloid dendritic cell
NA	neuraminidase
NAF	normal allantoic fluid
NIH	National Institutes of Health
OMe	methyl ester
OVA	ovalbumin
pDC	plasmacytoid dendritic cell
pfu	plaque-forming unit
ssRNA	single-stranded RNA
TLR	Toll-like receptor

References

1 Tamura, S., Tanimoto, T. and Kurata, T. 2005. Mechanisms of broad cross-protection provided by influenza virus infection and their application to vaccines. *Jpn J. Infect. Dis.* 58:195.
2 Doms, R. W., Helenius, A. and White, J. 1985. Membrane fusion activity of the influenza virus hemagglutinin. The low pH-induced conformational change. *J. Biol. Chem.* 260:2973.
3 Anders, H. J., Zecher, D., Pawar, R. D. and Patole, P. S. 2005. Molecular mechanisms of autoimmunity triggered by microbial infection. *Arthritis Res. Ther.* 7:215.
4 Diebold, S. S., Kaisho, T., Hemmi, H., Akira, S. and Reis e Sousa, C. 2004. Innate antiviral responses by means of TLR7-mediated recognition of single-stranded RNA. *Science.* 303:1529.
5 Dahl, M. E., Dabbagh, K., Liggitt, D., Kim, S. and Lewis, D. B. 2004. Viral-induced T helper type 1 responses enhance allergic disease by effects on lung dendritic cells. *Nat. Immunol.* 5:337.
6 Busch, R., Rinderknecht, C. H., Roh, S. *et al.* 2005. Achieving stability through editing and chaperoning: regulation of MHC class II peptide binding and expression. *Immunol. Rev.* 207:242.
7 Chapman, H. A. 1998. Endosomal proteolysis and MHC class II function. *Curr. Opin. Immunol.* 10:93.
8 Moss, C. X., Villadangos, J. A. and Watts, C. 2005. Destructive potential of the aspartyl protease cathepsin D in MHC class II-restricted antigen processing. *Eur. J. Immunol.* 35:3442.
9 Chain, B. M., Free, P., Medd, P., Swetman, C., Tabor, A. B. and Terrazzini, N. 2005. The expression and function of cathepsin E in dendritic cells. *J. Immunol.* 174:1791.
10 Bennett, K., Levine, T., Ellis, J. S. *et al.* 1992. Antigen processing for presentation by class II major histocompatibility complex requires cleavage by cathepsin E. *Eur. J. Immunol.* 22:1519.
11 Villadangos, J. A. and Ploegh, H. L. 2000. Proteolysis in MHC class II antigen presentation: who's in charge? *Immunity* 12:233.
12 Manoury, B., Hewitt, E. W., Morrice, N., Dando, P. M., Barrett, A. J. and Watts, C. 1998. An asparaginyl endopeptidase processes a microbial antigen for class II MHC presentation. *Nature* 396:695.
13 Shi, G. P., Villadangos, J. A., Dranoff, G. *et al.* 1999. Cathepsin S required for normal MHC class II peptide loading and germinal center development. *Immunity* 10:197.
14 Driessen, C., Lennon-Dumenil, A. M. and Ploegh, H. L. 2001. Individual cathepsins degrade immune complexes internalized by antigen-presenting cells via Fcgamma receptors. *Eur. J. Immunol.* 31:1592.
15 Watts, C. 1997. Capture and processing of exogenous antigens for presentation on MHC molecules. *Annu. Rev. Immunol.* 15:821.
16 Burster, T., Beck, A., Tolosa, E. *et al.* 2004. Cathepsin G, and not the asparagine-specific endoprotease, controls the processing of myelin basic protein in lysosomes from human B lymphocytes. *J. Immunol.* 172:5495.
17 Burster, T., Beck, A., Tolosa, E. *et al.* 2005. Differential processing of autoantigens in lysosomes from human monocyte-derived and peripheral blood dendritic cells. *J. Immunol.* 175:5940.

18 Trombetta, E. S., Ebersold, M., Garrett, W., Pypaert, M. and Mellman, I. 2003. Activation of lysosomal function during dendritic cell maturation. *Science* 299:1400.
19 Lautwein, A., Burster, T., Lennon-Dumenil, A. M. *et al.* 2002. Inflammatory stimuli recruit cathepsin activity to late endosomal compartments in human dendritic cells. *Eur. J. Immunol.* 32:3348.
20 Watts, C. 2004. The exogenous pathway for antigen presentation on major histocompatibility complex class II and CD1 molecules. *Nat. Immunol.* 5:685.
21 Sarawar, S. R., Sangster, M., Coffman, R. L. and Doherty, P. C. 1994. Administration of anti-IFN-gamma antibody to beta 2-microglobulin-deficient mice delays influenza virus clearance but does not switch the response to a T helper cell 2 phenotype. *J. Immunol.* 153:1246.
22 Maassab, H. F. and DeBorde, D. C. 1985. Development and characterization of cold-adapted viruses for use as live virus vaccines. *Vaccine* 3:355.
23 Schwarz, G., Boehncke, W. H., Braun, M. *et al.* 2002. Cathepsin S activity is detectable in human keratinocytes and is selectively upregulated upon stimulation with interferon-gamma. *J. Invest. Dermatol.* 119:44.
24 Greenbaum, D., Medzihradszky, K. F., Burlingame, A. and Bogyo, M. 2000. Epoxide electrophiles as activity-dependent cysteine protease profiling and discovery tools. *Chem. Biol.* 7:569.
25 Gilliet, M., Boonstra, A., Paturel, C. *et al.* 2002. The development of murine plasmacytoid dendritic cell precursors is differentially regulated by FLT3-ligand and granulocyte/macrophage colony-stimulating factor. *J. Exp. Med.* 195:953.
26 Greco, M. N., Hawkins, M. J., Powell, E. T. *et al.* 2002. Non-peptide inhibitors of cathepsin G: optimization of a novel beta-ketophosphonic acid lead by structure-based drug design. *J. Am. Chem. Soc.* 124:3810.
27 Chen, X., Reed-Loisel, L. M., Karlsson, L. and Jensen, P. E. 2006. H2-O expression in primary dendritic cells. *J. Immunol.* 176:3548.
28 Lennon-Dumenil, A. M., Bakker, A. H., Maehr, R. *et al.* 2002. Analysis of protease activity in live antigen-presenting cells shows regulation of the phagosomal proteolytic contents during dendritic cell activation. *J. Exp. Med.* 196:529.
29 Mizuochi, T., Yee, S. T., Kasai, M., Kakiuchi, T., Muno, D. and Kominami, E. 1994. Both cathepsin B and cathepsin D are necessary for processing of ovalbumin as well as for degradation of class II MHC invariant chain. *Immunol. Lett.* 43:189.
30 Katunuma, N., Matsunaga, Y., Matsui, A. *et al.* 1998. Novel physiological functions of cathepsins B and L on antigen processing and osteoclastic bone resorption. *Adv. Enzyme Regul.* 38:235.
31 Nishimura, Y., Kawabata, T. and Kato, K. 1988. Identification of latent procathepsins B and L in microsomal lumen: characterization of enzymatic activation and proteolytic processing *in vitro*. *Arch. Biochem. Biophys.* 261:64.
32 Hara, K., Kominami, E. and Katunuma, N. 1988. Effect of proteinase inhibitors on intracellular processing of cathepsin B, H and L in rat macrophages. *FEBS Lett.* 231:229.
33 Papini, E., de Bernard, M., Milia, E. *et al.* 1994. Cellular vacuoles induced by *Helicobacter pylori* originate from late endosomal compartments. *Proc. Natl Acad. Sci. USA* 91:9720.
34 Obermajer, N., Premzl, A., Zavasnik Bergant, T., Turk, B. and Kos, J. 2006. Carboxypeptidase cathepsin X mediates beta2-integrin-dependent adhesion of differentiated U-937 cells. *Exp. Cell Res.* 312:2515.
35 Kos, J., Sekirnik, A., Premzl, A. *et al.* 2005. Carboxypeptidases cathepsins X and B display distinct protein profile in human cells and tissues. *Exp. Cell Res.* 306:103.
36 Catalfamo, M. and Henkart, P. A. 2003. Perforin and the granule exocytosis cytotoxicity pathway. *Curr. Opin. Immunol.* 15:522.
37 Hermans, I. F., Ritchie, D. S., Yang, J., Roberts, J. M. and Ronchese, F. 2000. CD8+ T cell-dependent elimination of dendritic cells *in vivo* limits the induction of antitumor immunity. *J. Immunol.* 164:3095.
38 Cooper, A. and Shaul, Y. 2006. Clathrin-mediated endocytosis and lysosomal cleavage of hepatitis B virus capsid-like core particles. *J. Biol. Chem.* 281:16563.
39 Iwasaki, A. and Medzhitov, R. 2004. Toll-like receptor control of the adaptive immune responses. *Nat. Immunol.* 5:987.
40 Banchereau, J. and Steinman, R. M. 1998. Dendritic cells and the control of immunity. *Nature* 392:245.
41 Blander, J. M. and Medzhitov, R. 2006. Toll-dependent selection of microbial antigens for presentation by dendritic cells. *Nature* 440:808.
42 Marshall-Clarke, S., Tasker, L., Buchatska, O. *et al.* 2006. Influenza H2 haemagglutinin activates B cells via a MyD88-dependent pathway. *Eur. J. Immunol.* 36:95.
43 Kaznelson, D. W., Bruun, S., Monrad, A. *et al.* 2004. Simultaneous human papilloma virus type 16 E7 and cdk inhibitor p21 expression induces apoptosis and cathepsin B activation. *Virology* 320:301.
44 He, X. S., Draghi, M., Mahmood, K. *et al.* 2004. T cell-dependent production of IFN-gamma by NK cells in response to influenza A virus. *J. Clin. Invest.* 114:1812.
45 Katunuma, N., Matsunaga, Y., Himeno, K. and Hayashi, Y. 2003. Insights into the roles of cathepsins in antigen processing and presentation revealed by specific inhibitors. *Biol. Chem.* 384:883.
46 Maekawa, Y., Himeno, K., Ishikawa, H. *et al.* 1998. Switch of CD4+ T cell differentiation from Th2 to Th1 by treatment with cathepsin B inhibitor in experimental leishmaniasis. *J. Immunol.* 161:2120.
47 Nagaraj, N. S., Vigneswaran, N. and Zacharias, W. 2006. Cathepsin B mediates TRAIL-induced apoptosis in oral cancer cells. *J. Cancer Res. Clin. Oncol.* 132:171.